J Physiol Paris. Author manuscript; available in PMC 2015 August 07.

Published in final edited form as:

J Physiol Paris. 2008 ; 102(4-6): 195–208. doi:10.1016/j.jphysparis.2008.10.019.

Ionic and neuromodulatory regulation of burst discharge controls frequency tuning

W. Hamish Mehaffey[a,1], **Lee D. Ellis**[b,1], **Rüdiger Krahe**[c], **Robert J. Dunn**[b], and **Maurice J. Chacron**[d,*]

[a]Hotchkiss Brain Institute, University of Calgary, Calgary, Alberta, Canada T2N 4N1

[b]Center for Research in Neuroscience, McGill University, Montreal, QC, Canada H3G 1A4

[c]Department of Biology, McGill University, Montreal, QC, Canada H3A 1B1

[d]Department of Physiology and Physics, Center for Non-linear Dynamics, McGill University, McIntyre Medical Sciences Building, 3655 Promenade Sir William Osler, Montréal, Québec, Canada H3G 1Y6

Abstract

Sensory neurons encode natural stimuli by changes in firing rate or by generating specific firing patterns, such as bursts. Many neural computations rely on the fact that neurons can be tuned to specific stimulus frequencies. It is thus important to understand the mechanisms underlying frequency tuning. In the electrosensory system of the weakly electric fish, *Apteronotus leptorhynchus*, the primary processing of behaviourally relevant sensory signals occurs in pyramidal neurons of the electrosensory lateral line lobe (ELL). These cells encode low frequency prey stimuli with bursts of spikes and high frequency communication signals with single spikes. We describe here how bursting in pyramidal neurons can be regulated by intrinsic conductances in a cell subtype specific fashion across the sensory maps found within the ELL, thereby regulating their frequency tuning. Further, the neuromodulatory regulation of such conductances within individual cells and the consequences to frequency tuning are highlighted. Such alterations in the tuning of the pyramidal neurons may allow weakly electric fish to preferentially select for certain stimuli under various behaviourally relevant circumstances.

Keywords

Information theory; Weakly electric fish; Calcium dynamics; Neuromodulation; Acetylcholine; Bursting

1. Introduction

Sensory systems discriminate stimuli across multiple dimensions that can often vary across large intervals. As such, there is great interest in understanding the strategies used by sensory systems to respond to these large multi-dimensional natural stimulus ensembles

*Corresponding author. Tel.: +1 514 398 7493. maurice.chacron@mcgill.ca (M.J. Chacron).

[1]These authors contributed equally to this work.

(Abbott, 2005). One strategy would be to devote specific neural populations to encode different subsets of natural stimuli while another would be to have neural circuits that could alter the tuning of sensory neurons based on the behavioural context. Previous studies have found multiple maps of sensory space each with different tuning characteristics (MacLeod and Carr, 2007; Wässle, 2004). It has additionally been shown that sensory neurons receive large amounts of neuromodulatory input altering their excitability and responses to sensory input (Sarter et al., 2005). Thus, there is experimental evidence for both of these strategies.

One particularly relevant dimension of natural sensory input is the temporal frequency content of the signal. Frequency tuning has been demonstrated in the auditory (Elhilali et al., 2004) and visual (Butts et al., 2007; Priebe et al., 2006) and somatosensory (Andermann et al., 2004) systems. There is thus much interest in understanding the intrinsic biophysical and network mechanisms that contribute to shaping the frequency tuning of sensory neurons and the mechanisms by which it can be altered. In this manuscript, we review, and present new results on, the intrinsic mechanisms that determine the frequency tuning of sensory neurons within the electrosensory system of weakly electric fish as well as the mechanisms that regulate their expression.

The electrosensory system of *Apteronotus leptorhynchus* relies on perturbations of a self-generated electric field, the electric organ discharge (EOD), in order to sense its environment (Fig. 1A). Changes in the expected pattern of the EOD are caused by nearby objects, such as prey, and the EODs produced by conspecifics. While prey stimuli predominantly result in low frequency modulations in the amplitude of the electric organ discharge (EOD; Nelson and MacIver, 1999), conspecific related stimuli also contain high frequencies (Zupanc et al., 2006). Subcutaneous receptors respond to these modulations and relay this information to pyramidal cells within the electrosensory lateral line lobe (ELL).

We will first give a brief review of the relevant ELL anatomy and physiology related to frequency tuning. We then highlight some of our recent results on the effects of potassium channels on pyramidal cell frequency tuning, namely small conductance calcium-activated potassium channels (SK) and A-type potassium channels. Specifically, we have shown that A-type channels are modulated by cholinergic input, highlighting an important mechanism for the control of frequency responses. We then provide new results showing that activation of cholinergic pathways will lead to increased low frequency tuning through increased burst firing. Links between the two studies are proposed as the cholinergic pathways are also shown to regulate medium afterhyperpolarisations (mAHP's) in pyramidal neurons, suggesting that they may also affect small conductance calcium-activated potassium channels in addition to A-type potassium channels. The differential effects of cholinergic input on K^+ channels and their consequences on pyramidal cell frequency tuning are discussed and parallels to other systems are drawn.

2. Methods

2.1. In vivo electrophysiology

2.1.1. Recording—Extracellular recordings from pyramidal neurons were made with metal-filled micropipettes (Frank and Becker, 1964). Recording sites as determined from

surface landmarks and recording depth were limited to the centrolateral and lateral segments of the ELL only.

2.1.2. In vivo stimulation—The stimulation protocol was described previously in detail (Bastian et al., 2002; Chacron, 2006; Ellis et al., 2007a). Stimuli consisted of random amplitude modulations (RAM's) of the animal's own electric organ discharge (EOD) and were generated by multiplying a Gaussian band-limited (0–120 Hz, 8-th order Butterworth) white noise with an EOD mimic that consisted of a train of single-cycle sinusoids with frequency slightly higher than that of the EOD and phase locked to the zero-crossings of the animal's own EOD. The resulting signal was then presented via two silver/silver-chloride electrodes located 19 cm on each side of the animal, giving rise to stimuli that were spatially diffuse (Fig. 1B). Stimulus intensities were similar to those previously used and typical contrasts used ranged between 5% and 20%. Each stimulus presentation lasted 100 s in order to obtain sufficient amounts of data.

2.1.3. In vivo pharmacology—Previously established micropressure ejection techniques were used to focally apply drugs within the ELL dorsal molecular layer (DML) containing the apical dendritic trees of pyramidal cells (Bastian and Courtright, 1991; Bastian and Nguyenkim, 2001; Bastian et al., 2004; Chacron et al., 2005a, b; Chacron, 2006).

2.2. In vitro electrophysiology

Fish (*A. leptorhynchus*) were obtained from local importers and maintained at 26–28 °C in freshwater aquaria, in accordance with protocols approved by the McGill University Animal Care Committee. All chemicals were obtained from SIGMA (St. Louis, MO) unless otherwise noted. Animals were anaesthetized in 0.05% phenoxyethanol, and ELL tissue slices of 300–400 μm thickness were prepared, and recorded from, as previously described (Turner et al., 1994). For analysis of coherence or frequency content, RAMs were created as current injection protocols lasting 100 s, with frequency content between 0 and 60 Hz, as these frequencies are accurately represented in the pyramidal cell membrane voltage (Chacron et al., 2003a; Middleton et al., 2006). The current injections that we utilized are therefore a reasonable approximation of naturalistic sensory signals. These current waveforms were used to drive spiking in the cell, which could then be analysed similarly to the in vivo data (Fig. 1C), described in more detail below.

2.3. Modelling

A reduced two-compartment model was used to examine the effects of an I_A-like conductance on the firing behaviour of the cell based on previous models of the ELL pyramidal cell (Doiron et al., 2002; Fernandez et al., 2005b). The model consisted of a somatic and a dendritic compartment, each with Na^+, K^+, and leak currents. The dendrite further incorporates an inactivating K^+ current to mimic I_A. Full details of the model can be found in (Ellis et al., 2007a).

2.4. Data analysis

Data were analyzed using Clampfit 9.0 software (Molecular Devices, Palo Alto, CA) or Matlab R2006a (Mathworks, Natick, MA). Burst fractions were the proportion of interspike

intervals (ISIs) that were <10 ms, representing a previously defined burst threshold (Oswald et al., 2004). We obtained a binary sequence X(t) from the spike train sampled a 2 kHz. X(t) and the stimulus S(t) (also sampled at 2 kHz) were then used to calculate the stimulus-response coherence $C(f) = |P_{rs}(f)|^2/[P_{ss}(f)\ P_{rr}(f)]$ (Roddey et al., 2000). Here, P_{rs} denotes the stimulus-response cross spectrum, P_{ss} is the power spectrum of the stimulus, and P_{rr} is the power spectrum of the spike train. All spectral quantities were estimated using multitaper estimation techniques (Jarvis and Mitra, 2001). Note that the stimulus-response coherence directly relates to the mutual information measures we use in other papers (Chacron et al., 2005b; Ellis et al., 2007a), as: $I(f) = -\log2[1-C(f)]$ (in bits/s/Hz) (Borst and Theunissen, 1999). All values are reported as mean ± standard error. Further details can be found elsewhere (Ellis et al., 2007a,b). In order to quantify the frequency response, we computed the coherence between the stimulus and the resulting spike trains and then calculated a coherence ratio (ratio of the area under the coherence curve between 30 and 50 Hz to that under 0 and 20 Hz).

3. Review of relevant ELL anatomy and physiology

3.1. Anatomy

Cutaneous electroreceptors detect and encode the AMs generated by natural stimuli and project to pyramidal neurons in the hindbrain ELL (Turner and Maler, 1999). Pyramidal neurons are the sole AM processing output neurons of the ELL. These cells project to the torus semicircularis, which is analogous to the mammalian inferior colliculus (Maler, 1979; Maler et al., 1981). There are two types of pyramidal cells within the ELL: E cells are excited by increases in EOD amplitude and possess basilar dendrites, while I cells are inhibited by increases in EOD amplitude and lack basilar dendrites (Maler, 1979; Saunders and Bastian, 1984). These two main classes of cells can thus easily be separated in terms of anatomy alone. The ELL is divided into four segments: the medial segment receives input from ampullary electroreceptors and will not be further discussed here. The three other segments (centromedial-CMS; centrolateral-CLS, lateral-LS) all receive identical inputs from tuberous electroreceptors. Each segment is further organized in a laminar pattern with three distinct classes of pyramidal cells (superficial, intermediate and deep) named on the basis of the position of their somata within the pyramidal cell layer and characterized by differing morphologies (Bastian et al., 2004; Bastian and Nguyenkim, 2001; Chacron et al., 2005b). Pyramidal cells also receive massive amounts of feedback from higher centers (Maler, 1979).

3.2. Pyramidal cell frequency tuning

The electrosensory system of *A. leptorhynchus* is well adapted to detect AMs arising from both communication signals and from the relative motion of prey. This requires tuning to AM frequencies ranging from ~1 to 300 Hz (Benda et al., 2005; Benda et al., 2006; Nelson and MacIver, 1999) and spatial frequencies of 0.2–2 cycles/cm (Nelson and MacIver, 1999). These AM frequencies have specific behavioural relevance, because prey cause only low-frequency signals, whereas communication signals can extend to high frequencies. Pyramidal cell responses to time-varying inputs have been well characterized both in vitro (Berman and Maler, 1998a,b,c) and in vivo (Bastian, 1981, 2002; Chacron, 2006; Chacron

and Bastian, 2008; Chacron et al., 2003a; Chacron et al., 2005a). In particular, while receptor afferents generally respond equally well to all frequencies (Chacron et al., 2005a,b), pyramidal cells are generally tuned to a given range of frequencies (Bastian, 1981; Bastian et al., 2002; Chacron, 2006; Chacron et al., 2003b, 2005b; Krahe et al., 2002; Metzner et al., 1998; Shumway, 1989b). Previous studies have shown important differences in tuning between pyramidal cells of the different segments (Shumway, 1989a): pyramidal cells of the CMS/CLS/LS segments are tuned to low, mid, and high frequencies, respectively. This suggests a specific function for each segment, which has been partially verified through behavioural experiments (Metzner and Juranek, 1997). The mechanisms underlying differential tuning across the segments are still unclear. One hypothesis is that differences of intrinsic cellular properties could control tuning, while another is that network mechanisms are responsible. Recent evidence has shown differential expression of intrinsic conductances amongst the segments. For example, N-methyl-D-aspartate (NMDA) receptors are differentially expressed across the segments (Harvey-Girard et al., 2007). These receptors are thought to be involved in ELL plasticity required for adaptive cancellation of redundant stimuli (Bastian, 1999). Feedback input has been shown to significantly influence pyramidal cell dynamics as well as frequency tuning (Bastian et al., 2004; Chacron, 2006; Chacron and Bastian, 2008; Chacron et al., 2005b; Doiron et al., 2003). The respective roles of intrinsic membrane conductances and network mechanisms in determining pyramidal cell responses to sensory input are not fully understood, although the results presented here begin to clarify the possible functions.

3.3. Regulation of pyramidal cell bursting

Pyramidal cells have a well-characterized intrinsic burst mechanism that relies on a somato-dendritic interaction (Fernandez et al., 2005b; Lemon and Turner, 2000). Burst firing is driven by a depolarizing afterpotential (DAP) generated by current flowing back to the soma from actively back-propagating dendritic Na^+ spikes. The dendritic origin of the DAP can be revealed by blocking dendritic sodium channels with the application of TTX to the apical dendrites, eliminating the dendritic spike (Fernandez et al., 2005b; Mehaffey et al., 2005, 2006; Turner et al., 1994). This burst mechanism has been shown to be controlled by a variety of intrinsic membrane conductances including persistent sodium currents (Doiron et al., 2003) and high-threshold potassium channels (Ellis et al., 2007b; Fernandez et al., 2005a; Mehaffey et al., 2006; Noonan et al., 2003; Rashid et al., 2001a,b). As channel densities have been shown to vary across the different tuberous maps (Deng et al., 2005; Smith et al., 2006), they may contribute to map-specific computations including frequency selectivity (Metzner and Juranek, 1997; Shumway, 1989a). Furthermore, synaptic input from feedback pathways can have a significant impact on burst firing (Bastian and Nguyenkim, 2001; Chacron and Bastian, 2008; Chacron et al., 2005a; Mehaffey et al., 2007, 2008a).

Previous studies have suggested that ELL pyramidal cells can respond to afferent input in a frequency-dependent manner: spike bursts code preferentially for low frequency signals and isolated spikes code over a broad frequency range when stimulated with noise current injection (Oswald et al., 2004, 2007). In vivo intracellular recordings (Chacron et al., 2005b; Middleton et al., 2006) have demonstrated that a pyramidal cell's membrane potential can faithfully track synaptically transmitted sensory input within a broad frequency range (0–60

Hz). The in vitro current injections are therefore a reasonable approximation of naturalistic sensory signals.

4. SK2 channels contribute to tuning differences observed across the segments

Small conductance calcium-activated potassium (SK) channels (Ellis et al., 2007b) open in response to elevations in calcium and produce a medium after-hyperpolarization (mAHP) (Kohler et al., 1996; Sah and Faber, 2002). SK channels can regulate numerous aspects of neuronal dynamics including: spike frequency adaptation (Pedarzani et al., 2005), dendro-somatic coupling (Cai et al., 2004), as well as synaptic integration and potentiation (Faber et al., 2005; Ngo-Anh et al., 2005). The links between SK channel kinetics and behaviourally relevant neuronal computations have only recently begun to be examined for the SK2 subtype (Ellis et al., 2007b). In the following, we highlight some recent results on the role played by these channels in determining pyramidal cell dynamics and frequency tuning.

4.1. AptSK2 gene expression is regulated in a map specific manner

In situ hybridization was used to characterize *Apt*SK2 mRNA levels in pyramidal neurons of the three ELL segments showing strong labelling in both CLS and LS (Fig. 2A,B). Labelling of the CMS appeared to be weaker with fewer positive neurons overall. In the LS and CLS, both superficial and intermediate pyramidal neurons were strongly stained along with several classes of interneurons (granular cells and VML neurons; Fig. 2B). In the CMS, the expression of *Apt*SK2 mRNA showed further restriction; intermediate pyramidal neurons alone were labelled while adjacent superficial neurons appeared unlabelled.

Quantitative analyses showed that the levels of *in situ* hybridization signal for the *Apt*SK2 mRNA are low or even undetectable in all pyramidal neurons from the CMS superficial layer, while the other regions (CLS, LS and the intermediate cells of CMS) have 2 cell populations that are either strongly positive for *Apt*SK2 or do not express *Apt*SK2 mRNA (Fig. 2B). Further, the density of positively stained neurons was approximately half of the pyramidal cell density assessed from Nissl and Golgi stains (Maler, 1979). The *Apt*SK2 channels could thus be restricted to a particular pyramidal cell type (Ellis et al., 2007b).

4.2. Functional consequences of differential SK2 expression on the mAHP

The functional consequences of differential SK2 expression were investigated through in vitro electrophysiology. The effects of the SK channel blocker apamin and SK channel agonist EBIO were tested. It was found that apamin had a significant effect on both superficial and intermediate E cells of the LS and CLS by reducing the mAHP after an action potential (Fig. 3B).

In contrast, apamin had no effect on CMS superficial pyramidal cells (Fig. 3B), consistent with the lack of labelling observed with the *Apt*SK2 mRNA probe. Furthermore, SK channels were apparently expressed in labelled CMS intermediate E-type cells (Fig. 3B) where apamin again reduced the AHP. Application of the SK agonist EBIO had significant effects only in E-type pyramidal cells of the LS and CLS and on intermediate CMS E cells.

I-type pyramidal neurons of any segment were unaffected by application of either apamin or EBIO (Fig. 3C). Thus, the measurements of both apamin and EBIO effects on the AHPs confirmed the results of the mRNA localization study (Ellis et al., 2007b).

4.3. Functional consequences of differential SK2 expression on burst firing

Pyramidal cell burst firing patterns before and after SK channel modulation by either apamin or EBIO were quantified using the coefficient of variation (CV) of the interspike intervals (ISI). The CV provides a measure of the variability of spike discharge in response to step depolarizations and a CV of ≅1 is indicative of random firing (Poisson process with exponentially distributed ISIs (Bair et al., 1994; Softky and Koch, 1993)), while a CV≫1 is typically associated with burst discharge (Wilbur and Rinzel, 1983), allowing this measure to serve as a sensitive burst indicator. We note that, while the CV measure is sensitive to changes in firing rate, increases/decreases in firing rate have been shown to cause a decrease/increase in CV (Goldberg et al., 1984).

Application of EBIO regularized the discharge pattern as the CV was significantly decreased (1.1 ± 0.6 to 0.4 ± 0.4; Fig. 4A). The ISI histogram for the cell in Fig. 4 also revealed a dramatic shift to higher ISI values in response to EBIO, completely eliminating the shorter ISIs present in the original firing pattern (Fig. 4B). In contrast, apamin led to an increase in CV values (from 0.96 ± 0.12 to 1.77 ± 0.22). Predictably, for a given current step EBIO caused a decrease in firing rate while apamin caused an increase. However, we note that the changes in CV expected from changes in firing rate were opposite to those actually observed. We therefore take the changes in CV to be indicative of increased burst firing. For apamin, the increased tendency for burst firing was also apparent when the ISI values were plotted as a joint interval return map (Fig. 4B), further confirming our observations. In these maps, a tightly clustered group at short intervals combined with points along the X and Y axes stretching out to longer intervals represents burst firing (Turner et al., 1996).

As such, modulation of the mAHP by SK2 channels had a strong effect on the DAP mediated burst mechanism found in pyramidal cells. This occurs because the *Apt*SK2 mediated mAHP, by reducing the influence of the DAP that drives burst firing, can inhibit burst responses in the SK positive ELL pyramidal cells (Ellis et al., 2007b). Attenuation of the mAHP by apamin strongly enhances burst firing while enhancement by EBIO strongly attenuates burst firing (Fig. 4A,B).

4.4. Consequences of differential SK2 expression on frequency tuning

The ability for SK channels to regulate burst firing in some classes of pyramidal neurons suggested that they may modulate the computations performed by these neurons and in particular their frequency tuning. In vitro studies revealed that E cells of the CLS and LS segments could be broadband to high-pass in their coherence to noise current injections (a representative broadband cell is shown in Fig. 5A) (Ellis et al., 2008; Mehaffey et al., 2008b). In contrast, the superficial E cells in the CMS as well as I cells (representative cell is shown in Fig. 5B) were tuned to low frequencies. Cells that were sensitive to apamin and EBIO were thus tuned to higher frequencies than cells which were not. This suggests that SK channels make a strong contribution towards pyramidal cell frequency tuning. Pyramidal

cells were thus divided into an SK group and a non-SK group. In addition cells within the non-SK group had a higher tendency to burst than cells within the SK group (Ellis et al., 2007b).

Application of apamin on cells within the non-SK group did not bring about significant changes in either the response to the current injection or the tendency to burst (Fig. 5B). However, when apamin was applied to the SK group, the tuning of these cells to low frequency input increased while their tendency to burst also increased (Figs. 4 and 5). In order to evaluate whether the apamin induced increase in bursting (SK group) was responsible for the improvement in response to low frequency input, we first separated the spike train into bursts and isolated spikes based on an ISI threshold of 10 ms (Fig. 5C,D; broadband cell from Fig. 5A). We then computed coherence estimates for both bursts and isolated spikes as previously described (Oswald et al., 2004). The increase in burst fraction was associated with an increase in the mean burst coherence of the low-frequency component of the input (0–20 Hz; Fig. 5E). The isolated spike coherence remained unchanged (Fig. 5F) and isolated spikes coded equally well for all frequencies.

4.5. Summary and discussion

4.5.1. Contribution of SK2 channels to differential frequency tuning amongst the segments—The results described show that SK channels can have a significant influence on both burst firing as well as frequency tuning in vitro. It is thus highly probable that the differential distribution of SK channels across the segments contributes to the observed differences in frequency tuning amongst the segments in vivo. Recent in vitro results have shown differential pyramidal cell tuning to noise current injections that were strikingly similar to those observed in vivo (Mehaffey et al., 2008b), suggesting that the differential frequency tuning observed across the segments results mostly from differential expression of intrinsic membrane mechanisms rather than network effects. Nevertheless, further studies are needed to determine the actual extent to which SK channels and other intrinsic mechanisms actually contribute to differential frequency tuning.

4.5.2. Putative role of SK1 channels in frequency tuning—The results presented concentrated exclusively on SK2 channels, which were localized at the soma. SK1 channels have also been found in the ELL with differential expression across the segments increasing from CMS to LS in a similar fashion to SK2 channels (Ellis et al., 2008). However, SK1 channels were found to be localized in the dendrites and seem to be expressed in both E and I cells (Ellis et al., 2008). Further studies are needed to uncover the function of these channels. In particular, these channels could exert a strong influence on frequency tuning by affecting burst firing through the modulation of the back-propagating spike and thus the DAP.

5. Modulating ELL pyramidal cell responses to natural stimuli through regulation of intrinsic membrane conductances

Previous studies have shown that ELL pyramidal cells receive massive amounts of neuromodulatory input. In particular, cholinergic input has been demonstrated by the

presence of acetylcholinesterase as well as muscarinic receptors (Maler et al., 1981; Phan and Maler, 1983). ELL pyramidal cells also receive serotonergic input and previous studies have shown differential serotonin immunoreactivity across the segments (Johnston et al., 1990). Finally, pyramidal cells also receive noradrenergic input (Maler and Ellis, 1987), Such a wide range of neuromodulatory agents is likely to allow a, possibly complex, modulation of the computations performed by the ELL. Specifically, neuromodulators could regulate pyramidal cell frequency tuning based on the behavioural context. The following questions are then of particular importance: 1) How do neuromodulatory inputs affect ELL pyramidal cell frequency tuning? 2) What are the cellular mechanisms by which this occurs? 3) Under what behavioural contexts are these inputs active? In the following section, we will review some recent results on the cholinergic pathway and attempt to give partial answers to these important questions in the context of the electrosensory system.

5.1. Activation of cholinergic input unto pyramidal cells increases burst firing

Activation of cholinergic receptors in the ELL was achieved in vivo by injecting the agonist carbachol within the DML of the ELL where cholinergic binding sites are known to be located (Phan and Maler, 1983). In all cases, this led to a increase in firing rate (Fig. 6A) that recovered to control conditions (Ellis et al., 2007a), and was accompanied by a concomitant increase in burst firing that also recovered to control conditions (Fig. 6B). Carbachol is a non-selective agonist and will activate both nicotinic and muscarinic acetylcholine receptors. We found that the effects of carbachol on ELL pyramidal cells examined here were mediated exclusively by muscarinic receptor activation as atropine, a selective muscarinic antagonist, occluded the effects of carbachol (Ellis et al., 2007a).

5.2. Activation of cholinergic input unto pyramidal cells increases tuning to low frequencies in vivo

The consequences of such modulation in burst firing on frequency tuning were investigated under sensory stimulation with RAMs of the animal's own electric field that were spatially diffuse, mimicking distortions caused by conspecifics (see Fig. 1B; (Bastian et al., 2002; Chacron et al., 2003a, 2005b). Application of carbachol led to an increase in the stimulus-response coherence for frequencies of less than 40 Hz (compare black lines in Fig. 7A,B), which confirms interpretations based on mutual information results in our recent work (Ellis et al., 2007a), as well as an increase in burst firing. In order to ascertain whether the increase in low frequency coherence was due to increased burst firing, we segregated the spike train into bursts and isolated spikes and computed coherence estimates for both bursts and isolated spikes as previously described (Oswald et al., 2004). Similar to our observations during the blockade of SK channels, the increase in low-frequency coherence was primarily due to an increase in the coherence between bursts of spikes and low-frequency stimulus events (<20 Hz, Fig. 7C). However, application of carbachol also led to a slight increase in the coherence between isolated spikes and some lower-frequency stimulus components (20–40 Hz, Fig. 7D). This apparent discrepancy may be due to a difference in the mechanisms by which bursting is regulated, or to a difference in the stimuli used. The stimulus in the SK study consisted of 0–60 Hz filtered white noise, while the carbachol studies used 0–120 Hz filtered white noise. The frequency content of the stimulus is known to interact with the intrinsic burst mechanism (Doiron et al., 2007; Oswald et al., 2007), and may therefore

contribute to part of the observed difference between burst segregation in the two conditions. Regardless of the relative contributions of these mechanisms, we conclude that activation of cholinergic input onto pyramidal cells can increase their response to low frequency sensory stimuli, similar to our apamin blockade experiments above. This suggests a common mechanism, by which low frequency coherence is increased via an increase in burst firing.

5.3. Application of carbachol in vitro increases burst firing

Muscarinic receptor activation has been found to alter the firing properties of individual neurons through the modulation of a number of individual ionic conductances (Chen and Johnston, 2004; Delgado-Lezama et al., 1997; Stocker et al., 1999). In order to determine if the effects of mAChR activation resulted from the regulation of one or several ion channels, we used an in vitro ELL slice preparation (Turner et al., 1994, 1996).

It was found that carbachol applied to the DML resulted in a depolarization of the membrane potential from rest, which could cause the cell to cross the spiking threshold (Fig. 6C). This effect was mediated by muscarinic receptors as application of atropine prior to carbachol occluded this effect (Fig. 6D). Step current injections revealed an increase in firing rate following carbachol as well as an increase in burst firing (Fig. 6E and F). The effects of carbachol on the in vitro slice preparations were thus found to be qualitatively similar to those obtained in vivo (Ellis et al., 2007a).

5.4. Down-regulation of a 4-AP sensitive K^+ current by muscarinic input

The membrane depolarization caused by carbachol application in vitro (Fig. 6C) suggests an effect on subthreshold membrane properties, as opposed to the spiking dynamics. Carbachol increased the membrane resistance by ~25% thus suggesting the removal of a subthreshold outward current such as a K^+ channel (Ellis et al., 2007a). We then hypothesized that subthreshold K^+ currents were responsible for the effects of carbachol.

In ELL pyramidal neurons, a 4-AP sensitive A-type subthreshold K^+ current was previously shown to control the first spike latency following a step depolarization (Mathieson and Maler, 1988). The initial period before spiking is controlled by the membrane potential value preceding depolarization. More hyperpolarized levels can remove the inactivation of I_A and thereby increase first spike latency (Connor and Stevens, 1971; McCormick, 1991; Schoppa and Westbrook, 1999). A similar voltage dependence of first spike latency was shown for some ELL pyramidal neurons (Mathieson and Maler, 1988). It was found that carbachol significantly shortened the first spike latency after a step depolarization (Fig. 8A), thereby suggesting that muscarinic receptor activation leads to a down-regulation of the A current. This hypothesis was supported through experiments involving 4-AP, a known A-type current blocker, as well as TEA, a potent blocker of high-threshold potassium currents. We found that 4-AP led to a membrane potential depolarization similar to that observed with carbachol application as well as a decrease in the first spike latency (Fig. 8B). Conversely, first spike latency was not affected by TEA (Fig. 8C), but could be reduced by a subsequent application of carbachol (Fig. 8D). We therefore conclude that carbachol's effects can be mimicked, and occluded by 4-AP, but not TEA, suggesting carbachol acts via the effects of mAChR

activation on a 4-AP sensitive, TEA insensitive, subthreshold K^+ current, such as I_A (Fig. 8E).

The removal of an A-type current from a previously built model (Doiron et al., 2002) could reproduce all the effects observed in vitro: the membrane depolarization, the decreased first spike latency, as well as increases in firing rate and burst firing (Ellis et al., 2007a).

It is however possible that muscarinic input could also be simultaneously regulating other conductances. In the following section, we present some new results showing muscarinic modulation of the AHP which mediates many aspects of the ELL pyramidal cell's firing behaviour as seen previously (Ellis et al., 2007b; Fernandez et al., 2005a; Mehaffey et al., 2005).

5.5. Neuromodulatory regulation of AHPs

Our results show that the AHP following each spike was reduced by carbachol (decrease of 2.57 mV ± 0.209, Fig. 9A,C). There was no associated change in spike half-width (0.044 ms ± 0.01 ms), but a small reduction in spike height (4.9 ± 0.74 mV) also associated with the application of carbachol (Fig. 9D,E).

In order to see whether such effects could be explained by the down-regulation of A-type K^+ currents, we compared the AHP with and without I_A in a model pyramidal neuron (see Section 2). Interestingly, we were unable to reproduce the magnitude of the decrease in AHP height (Fig. 9E), causing a decrease in the AHP of <1 mV. This suggests that the change in AHP amplitude is not completely explained by a down-regulation of I_A and therefore that other currents are affected.

There is strong evidence in other systems that the expression A-type channels shows a gradient of expression within dendritic regions increasing in density farther from the soma (Hoffman et al., 1997; Johnston et al., 1996). When the gradient of I_A is removed pharmacologically (Hoffman et al., 1997) or is knocked down (Chen et al., 2006) the amplitude (and thus the potential somatic influence) of back-propagating spikes is increased. Further, this may increase the width of the back-propagating spike, leading to an increase of the DAP which will counteract the AHP, thereby increasing somatic excitability. Alternatively, mAChR activation might also down-regulate high-threshold K^+ currents such as Kv3.3 (Rashid et al., 2001a) or SK1 channels (Ellis et al., 2008), which have been found in pyramidal cell dendrites, and which can regulate burst firing (Noonan et al., 2003). The similarity between the effects of carbachol and those of apamin on the AHP (Figs. 3 and 9) suggest that carbachol may also down-regulate SK channels. Regulation of this AHP may play a crucial role in establishing the firing behaviour of the cell, including it's gain (Mehaffey et al., 2005; Troyer and Miller, 1997), and it's frequency-selectivity (Ellis et al., 2007b; Mehaffey et al., 2008b).

5.6. Summary and discussion

In this section, we reviewed recent results showing the effects of muscarinic receptor activation. Such activation can alter ELL pyramidal cell frequency tuning in vivo through increases in burst firing. Complementary in vitro studies revealed that muscarinic receptor

activation could alter cell excitability and burst firing through the down-regulation of an A-type K^+ current.

5.6.1. Potential mechanisms by which muscarinic receptor activation could down-regulate the AHP—We have presented new results showing that muscarinic receptor activation can modulate the AHP, although the particular mechanisms by which this is achieved remain to be elucidated. On the one hand, there is strong evidence in other systems that the expression A-type channels increases in dendritic regions that are farther from the soma (Hoffman et al., 1997; Johnston et al., 1996), which may decrease the width of the back-propagating spike, leading to an decrease of the DAP that opposes the AHP, thereby decreasing somatic excitability. Blocking these channels would then increase the DAP and decrease the AHP. Alternatively, mAChR activation might also down-regulate high-threshold K^+ currents such as Kv3.3 (Rashid et al., 2001a) or SK1 channels (Ellis et al., 2008) found in pyramidal cell dendrites, and which can regulate burst firing (Noonan et al., 2003). The similarity between the effects of carbachol and those of apamin on the AHP (Figs. 3 and 9) additionally suggests that carbachol may down-regulate SK channels. Since the regulation of the AHP may play a crucial role in establishing the firing behaviour of the cell, including it's gain (Mehaffey et al., 2005; Troyer and Miller, 1997), and it's frequency-selectivity (Ellis et al., 2007b; Mehaffey et al., 2008b), the mechanisms by which it is controlled are of great interest.

5.6.2. Behavioural contexts and sensory stimuli that could lead to muscarinic receptor activation—While the results presented show that the cholinergic pathway can alter burst firing and frequency tuning through the down-regulation of intrinsic membrane conductances, the behavioural context under which this input is activated remains unknown. The fact that muscarinic receptor activation selectively increased the response to low frequency input suggests that such input would preferentially activate muscarinic receptors. Prey stimuli have been shown to predominantly contain low frequencies (Nelson and MacIver, 1999), and pyramidal cells have been shown to respond differentially to spatially global and to spatially restricted stimuli mimicking prey (Bastian et al., 2002, 2004; Chacron, 2006; Chacron and Bastian, 2008; Chacron et al., 2003a, 2005a,b). Alternatively, low frequency diffuse stimuli have been shown to cause a well-known behavioural response in weakly electric fish called the jamming avoidance response (Heiligenberg, 1991). Further studies are needed to uncover the behavioural contexts leading to muscarinic receptor activation.

5.6.3. The source of cholinergic inputs to the ELL—Cholinergic input unto pyramidal cells most likely originates from eurydendroid cells within the caudal lobe of the cerebellum (Phan and Maler, 1983; Maler et al., 1981; Mathieson and Maler, 1988; Berman and Maler, 1999). The circuitry within the caudal lobe of the cerebellum is similar to that of the deep cerebellar nuclei in mammalian systems (Finger, 1978). While the general morphology (Guest, 1983) and some of the cellular projections (Carr, 1986) of eurydendroid cells have been investigated, the sensory responsiveness of this cell type is unknown and may be activated by input from higher brain centers, similar to the cholinergic pathways in

mammalian systems. The results presented here make the analysis of this input pathway a critical component required to understand its effects on sensory processing.

6. Parallels with other systems

6.1. Multiple maps

Sensory systems are tuned to natural signals from the environment that have shaped their evolution. Since such signals often have widely different attributes (Simoncelli and Olshausen, 2001), sensory systems must have developed strategies to efficiently process them. One mechanism used to encode specific aspects of the signal involves multiple neuronal representations (‘maps’) that differentially encode the same stimulus, as found in the auditory and olfactory systems. This often involves gradients of expression of specific ion channels as observed in the ELL (Deng et al., 2005; Ellis et al., 2007b; Mehaffey et al., 2006; Smith et al., 2006) and in mammalian auditory processing, in particular in the auditory brainstem (Li et al., 2001; Perney and Kaczmarek, 1997; von Hehn et al., 2004).

We have focused here on our most recent results concerning calcium-activated K^+ currents which can regulate the burst dynamics of pyramidal neurons in a map-specific fashion (Ellis et al., 2007b). In addition we highlight the importance of individual conductances by showing their potential modulation by second messenger systems, such as those initiated by mAChR activation (Ellis et al., 2007a). In addition, we have shown that the increased low frequency response of pyramidal cells under mAchR activation was due to an increased burst response and that this activation led to a decrease in the AHP that was similar to that observed under apamin (Ellis et al., 2007b) or TEA (Rashid et al., 2001b). This led to the hypothesis that additional K^+ currents, such as SK channels or Kv3.3 channels in ELL pyramidal cells are under neuromodulatory control. We summarize the results on the differential expression of SK channels amongst segments and cell class in Fig. 10. Briefly, each map contains both E and I type pyramidal cells in approximately equal numbers, all of which appear to receive muscarinic inputs (Fig. 10A). The intrinsic frequency tuning of E cells generally increases laterally across maps, while the frequency tuning of I-type pyramidal cells is low-pass regardless of map (Ellis et al., 2008; Mehaffey et al., 2008b). This correlates with the expression pattern of SK channels, which are expressed in E cells in the two more lateral maps, but not in I cells (Ellis et al., 2008). A further restriction occurs within maps, with only intermediate E cells of the CMS expressing SK, while superficial E cells lack SK channels and display low-pass characteristics (Fig. 10B) (Ellis et al., 2008). SK currents appear to be expressed in both intermediate and superficial E cells in the LS and CLS (Fig. 10B). It remains unknown whether the third type of pyramidal cell (deep pyramidal cells) expresses SK channels, as staining in the GCL could be either granular cells, or deep pyramidal cells, and no electrophysiology was performed.

6.2. Bursts, burst regulation, and sensory processing

ELL pyramidal cells are not the only cells displaying both bursting and tonic modes of firing. Lateral geniculate nucleus neurons also have dual modes of firing and a review has highlighted the similarities between both systems (Krahe and Gabbiani, 2004). LGN relay cells have a well-characterized burst mechanism (Sherman, 2001), and in the LGN bursts

transmit information about low frequency stimuli (Lesica and Stanley, 2004) and select events from natural stimuli (Wang et al., 2007). The results presented here along with previous work showing an increase in burst firing can increase a neuron's response to low frequencies (Ellis et al., 2007a, b) are consistent with the results from the LGN. It is likely that control of frequency tuning through the regulation of K^+ currents will be found in other systems and it may be a general mechanism by which neural responses to sensory input are regulated. Enhanced processing of specific sensory information through changes in excitability by up or down-regulation of voltage or calcium dependent K^+ currents may be a common feature of sensory processing.

There may be numerous network and biophysical mechanisms that regulate the relative size of the DAP and mAHP in the electrosensory system, allowing them to control bursting and thus low frequency tuning. At the network level it has already been established in vivo that frequency tuning is controlled by feedback input to ELL pyramidal cells (Chacron et al., 2003a, 2005b). Further support for this comes from in vitro studies showing that the DAP amplitude and bursting can be regulated on a fast timescale by these feedback pathways (Mehaffey et al., 2005, 2007, 2008a). The necessity for cell-intrinsic regulation of bursting is suggested by the greater prominence of the DAP in LS (see Fig. 3A). Thus in order to prevent bursting in the LS a large opposing SK current would be required. However, as recently discussed (Izhikevich, 2007; Marder and Goaillard, 2006), the function of SK channels cannot be predicted from their dynamics alone. Rather, in this case, information transmission by ELL pyramidal cells likely depends on the complex dynamical interactions of at least SK channels (Ellis et al., 2007b), the DAP generated by the interaction between dendritic Na^+ channels (Fernandez et al., 2005b) and K^+ channels (Mehaffey et al., 2006; Noonan et al., 2003; Rashid et al., 2001b), somatic persistent Na^+ channels (Berman et al., 2001), feedback from fast synaptic inputs (Mehaffey et al., 2005, 2007), and A-type K^+ channels (Ellis et al., 2007a).

Acknowledgments

This research was supported by NSERC (R.K.), and CIHR (R.J.D., M.J.C.) operating grants. Studentships to W.H.M were provided by AHFMR and CIHR.

References

Abbott, LF. Where are the switches on this thing?. In: van Hemmen, JL., Sejnowski, TJ., editors. 23 Problems in Systems Neuroscience. Oxford University Press; 2005. p. 423-431.

Andermann ML, Ritt J, Neimark MA, Moore CI. Neural correlates of vibrissa resonance; band-pass and somatotopic representation of high-frequency stimuli. Neuron. 2004; 42:451–463. [PubMed: 15134641]

Bair W, Koch C, Newsome W, Britten K. Power spectrum analysis of bursting cells in area MT in the behaving monkey. J Neurosci. 1994; 14:2870–2892. [PubMed: 8182445]

Bastian J. Electrolocation II. The effects of moving objects and other electrical stimuli on the activities of two categories of posterior lateral line lobe cells in *Apteronotus albifrons*. J Comp Physiol [A]. 1981; 144:481–494.

Bastian J. Plasticity of feedback inputs in the apteronotid electrosensory system. J Exp Biol. 1999; 202(Pt 10):1327–1337. [PubMed: 10210673]

Bastian J, Courtright J. Morphological correlates of pyramidal cell adaption rate in the electrosensory lateral line lobe of weakly electric fish. J Comp Physiol. 1991; 168:393–407. [PubMed: 1865386]

Bastian J, Nguyenkim J. Dendritic modulation of burst-like firing in sensory neurons. J Neurophysiol. 2001; 85:10–22. [PubMed: 11152701]

Bastian J, Chacron MJ, Maler L. Receptive field organization determines pyramidal cell stimulus-encoding capability and spatial stimulus selectivity. J Neurosci. 2002; 22:4577–4590. [PubMed: 12040065]

Bastian J, Chacron MJ, Maler L. Plastic and nonplastic pyramidal cells perform unique roles in a network capable of adaptive redundancy reduction. Neuron. 2004; 41:767–779. [PubMed: 15003176]

Benda J, Longtin A, Maler L. Spike-frequency adaptation separates transient communication signals from background oscillations. J Neurosci. 2005; 25:2312–2321. [PubMed: 15745957]

Benda J, Longtin A, Maler L. A synchronization–desynchronization code for natural communication signals. Neuron. 2006; 52:347–358. [PubMed: 17046696]

Berman NJ, Maler L. Distal versus proximal inhibitory shaping of feedback excitation in the electrosensory lateral line lobe: implications for sensory filtering. J Neurophysiol. 1998a; 80:3214–3232. [PubMed: 9862917]

Berman NJ, Maler L. Inhibition evoked from primary afferents in the electrosensory lateral line lobe of the weakly electric fish (*Apteronotus leptorhynchus*). J Neurophysiol. 1998b; 80:3173–3196. [PubMed: 9862915]

Berman NJ, Maler L. Interaction of GABAB-mediated inhibition with voltage-gated currents of pyramidal cells: computational mechanism of a sensory searchlight. J Neurophysiol. 1998c; 80:3197–3213. [PubMed: 9862916]

Berman N, Dunn RJ, Maler L. Function of NMDA receptors and persistent sodium channels in a feedback pathway of the electrosensory system. J Neurophysiol. 2001; 86:1612–1621. [PubMed: 11600624]

Butts DA, Weng C, Jin J, Yeh CI, Lesica NA, Alonso JM, Stanley GB. Temporal precision in the neural code and the timescales of natural vision. Nature. 2007; 449:92–95. [PubMed: 17805296]

Cai X, Liang CW, Muralidharan S, Kao JP, Tang CM, Thompson SM. Unique roles of SK and Kv4.2 potassium channels in dendritic integration. Neuron. 2004; 44:351–364. [PubMed: 15473972]

Carr CE. Time coding in electric fish and barn owls. Brain Behav Evol. 1986; 28:122–133. [PubMed: 3567536]

Chacron MJ. Nonlinear information processing in a model sensory system. J Neurophysiol. 2006; 95:2933–2946. [PubMed: 16495358]

Chacron MJ, Bastian JA. Population coding by electrosensory neurons. J Neurophysiol. 2008; 100:852–867. [PubMed: 18509073]

Chacron MJ, Doiron B, Maler L, Longtin A, Bastian J. Non-classical receptive field mediates switch in a sensory neuron's frequency tuning. Nature. 2003a; 423:77–81. [PubMed: 12721628]

Chacron MJ, Longtin A, Maler L. The effects of spontaneous activity, background noise, and the stimulus ensemble on information transfer in neurons. Network. 2003b; 14:803–824. [PubMed: 14653504]

Chacron MJ, Longtin A, Maler L. Delayed excitatory and inhibitory feedback shape neural information transmission. Phys Rev E Stat Nonlin Soft Matter Phys. 2005a; 72:051917. [PubMed: 16383655]

Chacron MJ, Maler L, Bastian J. Feedback and feed forward control of frequency tuning to naturalistic stimuli. J Neurosci. 2005b; 25:5521–5532. [PubMed: 15944380]

Chen X, Johnston D. Properties of single voltage-dependent K^+ channels in dendrites of CA1 pyramidal neurones of rat hippocampus. J Physiol. 2004; 559:187–203. [PubMed: 15218076]

Chen X, Yuan LL, Zhao C, Birnbaum SG, Frick A, Jung WE, Schwarz TL, Sweatt JD, Johnston D. Deletion of Kv4.2 gene eliminates dendritic A-type K^+ current and enhances induction of long-term potentiation in hippocampal CA1 pyramidal neurons. J Neurosci. 2006; 26:12143–12151. [PubMed: 17122039]

Connor JA, Stevens CF. Voltage clamp studies of a transient outward membrane current in gastropod neural somata. J Physiol. 1971; 213:21–30. [PubMed: 5575340]

Delgado-Lezama R, Perrier JF, Nedergaard S, Svirskis G, Hounsgaard J. Metabotropic synaptic regulation of intrinsic response properties of turtle spinal motoneurones. J Physiol. 1997; 504(Pt 1):97–102. [PubMed: 9350621]

Deng Q, Rashid AJ, Fernandez FR, Turner RW, Maler L, Dunn RJ. A C-terminal domain directs Kv3.3 channels to dendrites. J Neurosci. 2005; 25:11531–11541. [PubMed: 16354911]

Doiron B, Chacron MJ, Maler L, Longtin A, Bastian J. Inhibitory feedback required for network oscillatory responses to communication but not prey stimuli. Nature. 2003; 421:539–543. [PubMed: 12556894]

Doiron B, Laing C, Longtin A, Maler L. Ghostbursting: a novel neuronal burst mechanism. J Comput Neurosci. 2002; 12:5–25. [PubMed: 11932557]

Doiron B, Oswald AM, Maler L. Interval coding. II. Dendrite-dependent mechanisms. J Neurophysiol. 2007; 97:2744–2757. [PubMed: 17409177]

Elhilali M, Fritz JB, Klein DJ, Simon JZ, Shamma SA. Dynamics of precise spike timing in primary auditory cortex. J Neurosci. 2004; 24:1159–1172. [PubMed: 14762134]

Ellis LD, Krahe R, Bourque CW, Dunn RJ, Chacron MJ. Muscarinic receptors control frequency tuning through the downregulation of an A-type potassium current. J Neurophysiol. 2007a; 98:1526–1527. [PubMed: 17615127]

Ellis LD, Maler L, Dunn RJ. Differential distribution of SK channel subtypes in the brain of the weakly electric fish *Apteronotus leptorhynchus*. J Comp Neurol. 2008; 507:1964–1978. [PubMed: 18273887]

Ellis LD, Mehaffey WH, Harvey-Girard E, Turner RW, Maler L, Dunn RJ. SK Channels provide a novel mechanism for the control of frequency tuning in electrosensory neurons. J Neurosci. 2007b; 27:9491–9502. [PubMed: 17728462]

Faber ES, Delaney AJ, Sah P. SK channels regulate excitatory synaptic transmission and plasticity in the lateral amygdala. Nat Neurosci. 2005; 8:635–641. [PubMed: 15852010]

Fernandez FR, Mehaffey WH, Molineux ML, Turner RW. High-threshold K^+ current increases gain by offsetting a frequency-dependent increase in low-threshold K^+ current. J Neurosci. 2005a; 25:363–371. [PubMed: 15647479]

Fernandez FR, Mehaffey WH, Turner RW. Dendritic Na^+ current inactivation can increase cell excitability by delaying a somatic depolarizing afterpotential. J Neurophysiol. 2005b; 94:3836–3848. [PubMed: 16120659]

Finger TE. Efferent neurons of the teleost cerebellum. Brain Res. 1978; 153:608–614. [PubMed: 81089]

Frank, K., Becker, MC. Physical techniques in biological research. Nastuk, WL., editor. Vol. 5. Academic Press; New York: 1964. p. 23-87.p. 239-243.

Goldberg JM, Smith CE, Fernandez C. Relation between discharge regularity and responses to externally applied galvanic currents in vestibular nerve afferents of the squirrel monkey. J Neurophysiol. 1984; 51:1236–1256. [PubMed: 6737029]

Harvey-Girard E, Dunn RJ, Maler L. Regulated expression of *N*-methyl-D-aspartate receptors and associated proteins in teleost electrosensory system and telencephalon. J Comp Neurol. 2007; 505:644–668. [PubMed: 17948874]

Heiligenberg, W. Neural Nets in Electric Fish. MIT Press; Cambridge, Mass: 1991.

Hoffman DA, Magee JC, Colbert CM, Johnston D. K^+ channel regulation of signal propagation in dendrites of hippocampal pyramidal neurons. Nature. 1997; 387:869–875. [PubMed: 9202119]

Izhikevich, EM. Dynamical Systems in Neuroscience: The Geometry of Excitability and Bursting. MIT Press; Cambridge, MA: 2007.

Jarvis MR, Mitra PP. Sampling properties of the spectrum and coherency of sequences of action potentials. Neural Comput. 2001; 13:717–749. [PubMed: 11255566]

Johnston D, Magee JC, Colbert CM, Cristie BR. Active properties of neuronal dendrites. Annu Rev Neurosci. 1996; 19:165–186. [PubMed: 8833440]

Johnston SA, Maler L, Tinner B. The distribution of serotonin in the brain of *Apteronotus leptorhynchus*: an immunohistochemical study. J Chem Neuroanat. 1990; 3:429–465. [PubMed: 2291814]

Kohler M, Hirschberg B, Bond CT, Kinzie JM, Marrion NV, Maylie J, Adelman JP. Small-conductance, calcium-activated potassium channels from mammalian brain. Science. 1996; 273:1709–1714. [PubMed: 8781233]

Krahe R, Gabbiani F. Burst firing in sensory systems. Nat Rev Neurosci. 2004; 5:13–23. [PubMed: 14661065]

Krahe R, Kreiman G, Gabbiani F, Koch C, Metzner W. Stimulus encoding and feature extraction by multiple sensory neurons. J Neurosci. 2002; 22:2374–2382. [PubMed: 11896176]

Lemon N, Turner RW. Conditional spike backpropagation generates burst discharge in a sensory neuron. J Neurophysiol. 2000; 84:1519–1530. [PubMed: 10980024]

Lesica NA, Stanley GB. Encoding of natural scene movies by tonic and burst spikes in the lateral geniculate nucleus. J Neurosci. 2004; 24:10731–10740. [PubMed: 15564591]

Li W, Kaczmarek LK, Perney TM. Localization of two high-threshold potassium channel subunits in the rat central auditory system. J Comp Neurol. 2001; 437:196–218. [PubMed: 11494252]

MacLeod KM, Carr CE. Beyond timing in the auditory brainstem: intensity coding in the avian cochlear nucleus angularis. Prog Brain Res. 2007; 165:123–133. [PubMed: 17925243]

Maler L. The posterior lateral line lobe of certain gymnotoid fish: quantitative light microscopy. J Comp Neurol. 1979; 183:323–363. [PubMed: 762262]

Maler L, Ellis WG. Inter-male aggressive signals in weakly electric fish are modulated by monoamines. Behav Brain Res. 1987; 25:75–81. [PubMed: 3620087]

Maler L, Sas EK, Rogers J. The cytology of the posterior lateral line lobe of high-frequency weakly electric fish (Gymnotidae): dendritic differentiation and synaptic specificity in a simple cortex. J Comp Neurol. 1981; 195:87–139. [PubMed: 7204653]

Marder E, Goaillard JM. Variability, compensation and homeostasis in neuron and network function. Nat Rev Neurosci. 2006; 7:563–574. [PubMed: 16791145]

Mathieson WB, Maler L. Morphological and electrophysiological properties of a novel in vitro preparation: the electrosensory lateral line lobe brain slice. J Comp Physiol [A]. 1988; 163:489–506.

McCormick DA. Functional properties of a slowly inactivating potassium current in guinea pig dorsal lateral geniculate relay neurons. J Neurophysiol. 1991; 66:1176–1189. [PubMed: 1761979]

Mehaffey WH, Doiron B, Maler L, Turner RW. Deterministic multiplicative gain control with active dendrites. J Neurosci. 2005; 25:9968–9977. [PubMed: 16251445]

Mehaffey WH, Fernandez FR, Rashid AJ, Dunn RJ, Turner RW. Distribution and function of potassium channels in the electrosensory lateral line lobe of weakly electric apteronotid fish. J Comp Physiol A Neuroethol Sens Neural Behav Physiol. 2006; 192:637–648. [PubMed: 16425062]

Mehaffey WH, Fernandez FR, Doiron B, Turner RW. Synaptic and dynamic regulation of pyramidal cell firing dynamics mediated by backpropating spikes. J Physiol Paris. 2008a

Mehaffey WH, Fernandez FR, Maler L, Turner RW. Regulation of burst dynamics improves differential encoding of stimulus frequency by spike train segregation. J Neurophysiol. 2007; 98:939–951. [PubMed: 17581845]

Mehaffey WH, Maler L, Turner RW. Regulation of intrinsic frequency tuning of ELL pyramidal cells across electrosensory maps. J Neurophysiol. 2008b

Metzner W, Juranek J. A sensory brain map for each behavior? Proc Natl Acad Sci USA. 1997; 94:14798–14803. [PubMed: 9405693]

Metzner W, Koch C, Wessel R, Gabbiani F. Feature extraction by burst-like spike patterns in multiple sensory maps. J Neurosci. 1998; 18:2283–2300. [PubMed: 9482813]

Middleton JW, Longtin A, Benda J, Maler L. The cellular basis for parallel neural transmission of a high-frequency stimulus and its low-frequency envelope. Proc Natl Acad Sci USA. 2006; 103:14596–14601. [PubMed: 16983081]

Nelson ME, MacIver MA. Prey capture in the weakly electric fish *Apteronotus albifrons*: sensory acquisition strategies and electrosensory consequences. J Exp Biol. 1999; 202:1195–1203. [PubMed: 10210661]

Ngo-Anh TJ, Bloodgood BL, Lin M, Sabatini BL, Maylie J, Adelman JP. SK channels and NMDA receptors form a Ca^{2+} mediated feedback loop in dendritic spines. Nat Neurosci. 2005; 8:642–649. [PubMed: 15852011]

Noonan L, Doiron B, Laing C, Longtin A, Turner RW. A dynamic dendritic refractory period regulates burst discharge in the electrosensory lobe of weakly electric fish. J Neurosci. 2003; 23:1524–1534. [PubMed: 12598641]

Oswald AM, Chacron MJ, Doiron B, Bastian J, Maler L. Parallel processing of sensory input by bursts and isolated spikes. J Neurosci. 2004; 24:4351–4362. [PubMed: 15128849]

Oswald AM, Doiron B, Maler L. Interval coding. I. Burst interspike intervals as indicators of stimulus intensity. J Neurophysiol. 2007; 97:2731–2743. [PubMed: 17409176]

Pedarzani P, McCutcheon JE, Rogge G, Jensen BS, Christophersen P, Hougaard C, Strobaek D, Stocker M. Specific enhancement of SK channel activity selectively potentiates the afterhyperpolarizing current *I*(AHP) and modulates the firing properties of hippocampal pyramidal neurons. J Biol Chem. 2005; 280:41404–41411. [PubMed: 16239218]

Perney TM, Kaczmarek LK. Localization of a high threshold potassium channel in the rat cochlear nucleus. J Comp Neurol. 1997; 386:178–202. [PubMed: 9295146]

Phan M, Maler L. Distribution of muscarinic receptors in the caudal cerebellum and electrosensory lateral line lobe of gymnotiform fish. Neurosci Lett. 1983; 42:137–143. [PubMed: 6664625]

Priebe NJ, Lisberger SG, Movshon JA. Tuning for spatiotemporal frequency and speed in directionally selective neurons of macaque striate cortex. J Neurosci. 2006; 26:2941–2950. [PubMed: 16540571]

Rashid AJ, Dunn RJ, Turner RW. A prominent soma-dendritic distribution of Kv3.3 K^+ channels in electrosensory and cerebellar neurons. J Comp Neurol. 2001a; 441:234–247. [PubMed: 11745647]

Rashid AJ, Morales E, Turner RW, Dunn RJ. The contribution of dendritic Kv3 K^+ channels to burst threshold in a sensory neuron. J Neurosci. 2001b; 21:125–135. [PubMed: 11150328]

Roddey JC, Girish B, Miller JP. Assessing the performance of neural encoding models in the presence of noise. J Comput Neurosci. 2000; 8:95–112. [PubMed: 10798596]

Sah P, Faber ES. Channels underlying neuronal calcium-activated potassium currents. Prog Neurobiol. 2002; 66:345–353. [PubMed: 12015199]

Sarter M, Hasselmo ME, Bruno JP, Givens B. Unraveling the attentional functions of cortical cholinergic inputs: interactions between signal-driven and cognitive modulation of signal detection. Brain Res Brain Res Rev. 2005; 48:98–111. [PubMed: 15708630]

Saunders J, Bastian J. The physiology and morphology of two types of electrosensory neurons in the weakly electric fish, *Apteronotus leptorhynchus*. J Comp Physiol [A]. 1984; 154:199–209.

Schoppa NE, Westbrook GL. Regulation of synaptic timing in the olfactory bulb by an A-type potassium current. Nat Neurosci. 1999; 2:1106–1113. [PubMed: 10570488]

Shumway CA. Multiple electrosensory maps in the medulla of weakly electric gymnotiform fish. I. Physiological differences. J Neurosci. 1989a; 9:4388–4399. [PubMed: 2593005]

Shumway CA. Multiple electrosensory maps in the medulla of weakly electric gymnotiform fish. II. Anatomical differences. J Neurosci. 1989b; 9:4400–4415. [PubMed: 2556508]

Simoncelli EP, Olshausen BA. Natural image statistics and neural representation. Annu Rev Neurosci. 2001; 24:1193–1216. [PubMed: 11520932]

Smith GT, Unguez GA, Weber CM. Distribution of Kv1-like potassium channels in the electromotor and electrosensory systems of the weakly electric fish *Apteronotus leptorhynchus*. J Neurobiol. 2006; 66:1011–1031. [PubMed: 16779822]

Softky WR, Koch C. The highly irregular firing of cortical cells is inconsistent with temporal integration of random EPSPs. J Neurosci. 1993; 13:334–350. [PubMed: 8423479]

Stocker M, Krause M, Pedarzani P. An apamin-sensitive Ca^{2+}-activated K^+ current in hippocampal pyramidal neurons. Proc Natl Acad Sci USA. 1999; 96:4662–4667. [PubMed: 10200319]

Troyer TW, Miller KD. Physiological gain leads to high ISI variability in a simple model of a cortical regular spiking cell. Neural Comput. 1997; 9:971–983. [PubMed: 9188190]

Turner RW, Maler L. Oscillatory and burst discharge in the apteronotid electrosensory lateral line lobe. J Exp Biol. 1999; 202:1255–1265. [PubMed: 10210666]

Turner RW, Maler L, Deerinck T, Levinson SR, Ellisman MH. TTX-sensitive dendritic sodium channels underlie oscillatory discharge in a vertebrate sensory neuron. J Neurosci. 1994; 14:6453–6471. [PubMed: 7965050]

Turner RW, Plant JR, Maler L. Oscillatory and burst discharge across electrosensory topographic maps. J Neurophysiol. 1996; 76:2364–2382. [PubMed: 8899610]

von Hehn CA, Bhattacharjee A, Kaczmarek LK. Loss of Kv3.1 tonotopicity and alterations in cAMP response element-binding protein signaling in central auditory neurons of hearing impaired mice. J Neurosci. 2004; 24:1936–1940. [PubMed: 14985434]

Wang X, Wei Y, Vaingankar V, Wang Q, Koepsell K, Sommer FT, Hirsch JA. Feedforward excitation and inhibition evoke dual modes of firing in the cat's visual thalamus during naturalistic viewing. Neuron. 2007; 55:465–478. [PubMed: 17678858]

Wässle H. Parallel processing in the mammalian retina. Nat Rev Neurosci. 2004; 5:747–757. [PubMed: 15378035]

Wilbur WJ, Rinzel J. A theoretical basis for large coefficient of variation and bimodality in neuronal interspike interval distributions. J Theor Biol. 1983; 105:345–368. [PubMed: 6656286]

Zupanc GK, Sirbulescu RF, Nichols A, Ilies I. Electric interactions through chirping behavior in the weakly electric fish, *Apteronotus leptorhynchus*. J Comp Physiol A Neuroethol Sens Neural Behav Physiol. 2006; 192:159–173. [PubMed: 16247622]

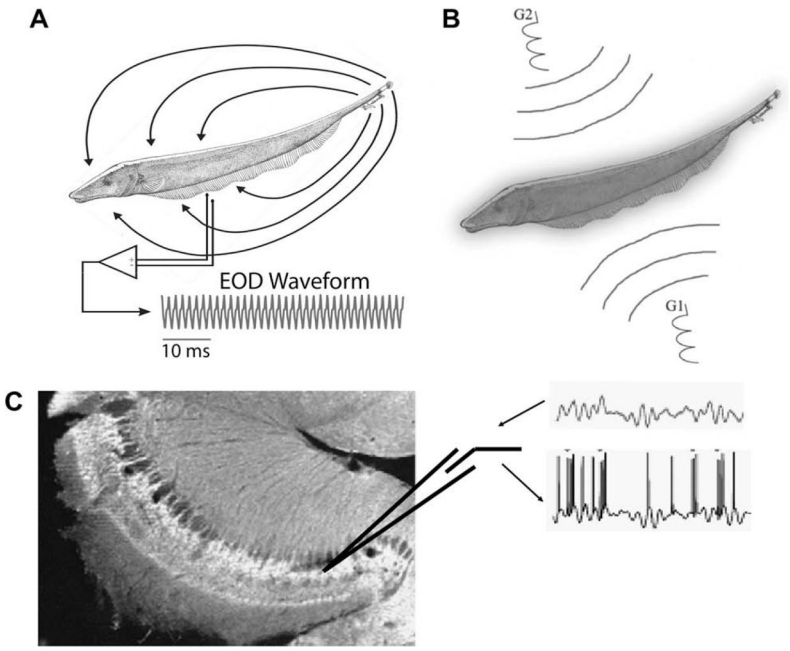

Fig. 1.

Recording and stimulation protocols. (A) Weakly electric fish generate an electric field around their body in order to electrolocate objects and for communication with conspecifics. For *Apteronotus leptorhynchus*, the EOD waveform recorded at one point in space is quasi-sinusoidal with a frequency of 600–1000 Hz. (B) Illustration of the Global stimulation geometry used. Amplitude modulations of the animal's own EOD are delivered via two silver/silver-chloride electrodes (G1 and G2) located 19 cm away on each side of the animal. The perturbations of the EOD created are roughly spatially homogeneous on the animal's skin surface. (C) Illustration of the in vitro stimulus preparations. AMs similar to those presented in vivo are translated to intracellular stimuli and used to drive pyramidal cells in vitro. Arrows indicate the presentation of an intracellular current stimulus and the recording of the spike train. These can then be analysed in a fashion similar to the in vivo recordings. DC current steps can also be applied.

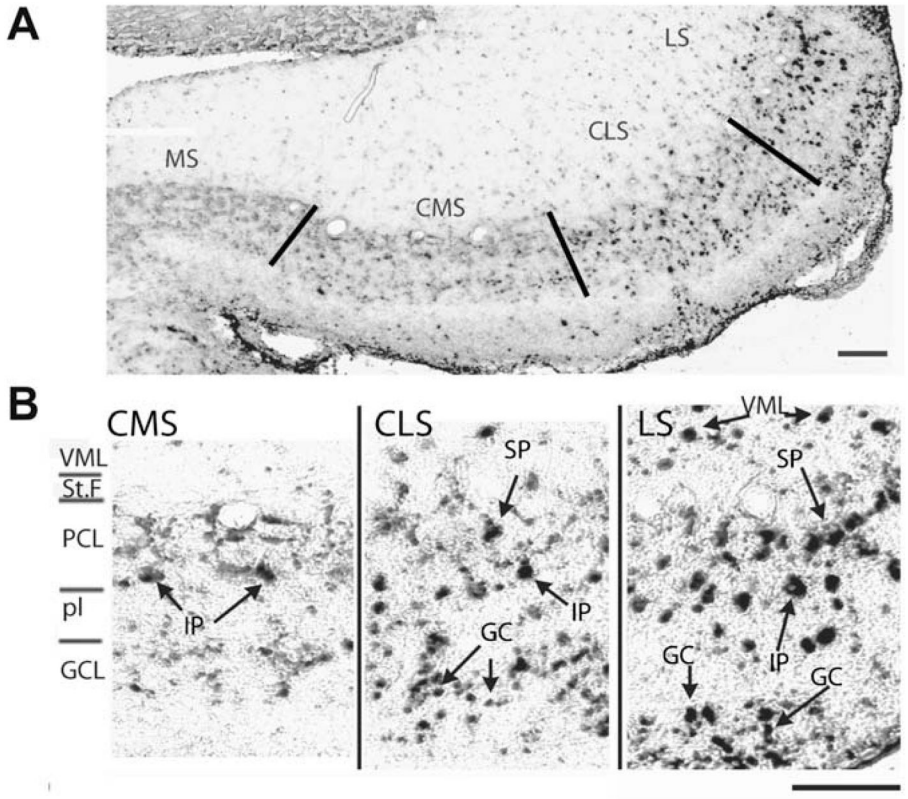

Fig. 2.

Segmental expression pattern of *Apt*SK2 in the ELL. (A) *In situ* hybridization analysis of *Apt*SK2 in the ELL. Lines indicate segment divisions of the sensory maps in the ELL. The highest expression is found in the lateral segment (LS), with a lower level found in the centrolateral (CLS) and centromedial segments (CMS). Levels were undetectable in the medial segment (MS). (B) Magnified view of the segmental localization pattern. Superficial (SP) and intermediate (IP) pyramidal neurons are strongly labelled in the LS and CLS along with ventral molecular layer (VML) interneurons and granule cells (GC). In the CMS only intermediate pyramidal neurons display strong SK2 expression. Scale bars: 100 μm. Modified from Ellis et al. (2007b).

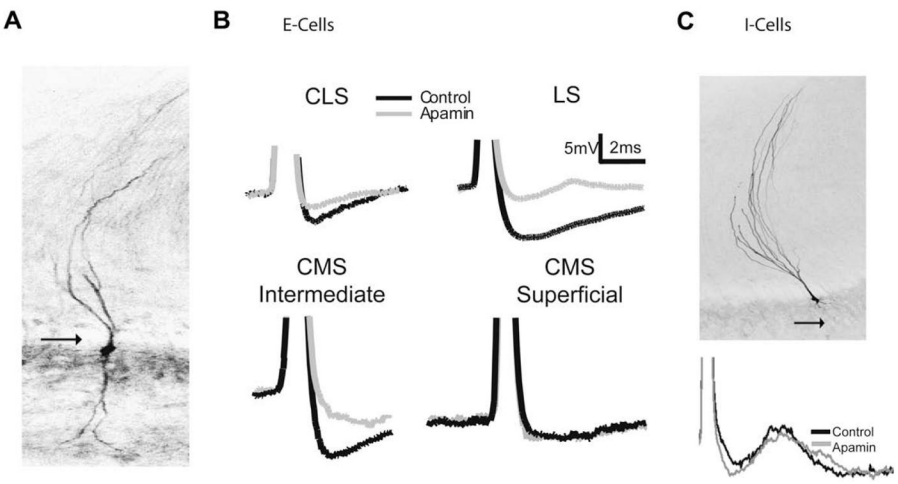

Fig. 3.

Apamin sensitivity varies with pyramidal cell subtype, and map. (A) An E cell labelled with neurobiotin showing the presence of a basilar dendrite (arrow). (B) Single cell AHP averages (n = ???) generated via intracellular current injection (0.1 nA) superimposed before and after drug treatment. Neurons in the LS, CLS along with CMS intermediate cells respond to apamin (grey) with a decrease in the size of the AHP. CMS superficial cells do not show a response to apamin. (C) Neurobiotin labelled I cell showing the lack of a basilar dendrite (arrow). Superimposed spike from an I cell showing no change in the AHP following apamin application. Modified from Ellis et al. (2007b).

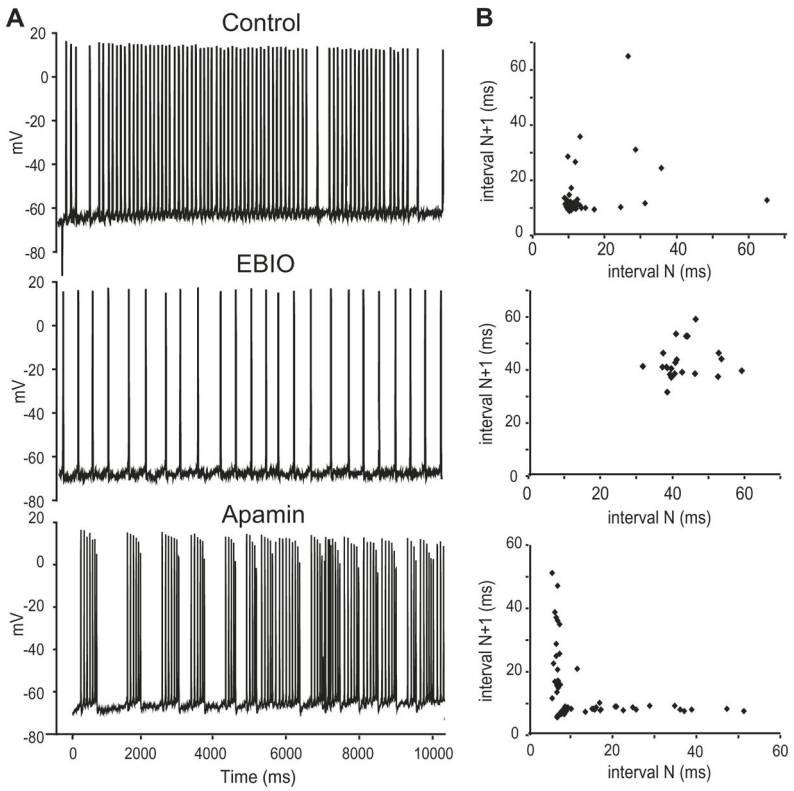

Fig. 4.

Activity of SK channels regulates bursting. (A) Representative traces from a CLS E cell (0.3nA current injection) showing a regularization of the firing pattern following EBIO (1 mM) and the subsequent conversion to a burst-firing mode following application of apamin (1 μM). (B) Joint interval return maps showing randomly distributed points under baseline conditions confirming a non-bursting firing mode; the shortest ISIs are typically >10 ms. EBIO leads to an increase in ISI values and a regularization that is demonstrated by the presence of a single cluster of long ISIs. Apamin leads to a separation of the return map into a burst cluster (ISIs < 10 ms) and broadly distributed longer ISI returns representing variable inter-burst intervals as previously shown by Turner et al. (1996). Modified from Ellis et al. (2007b).

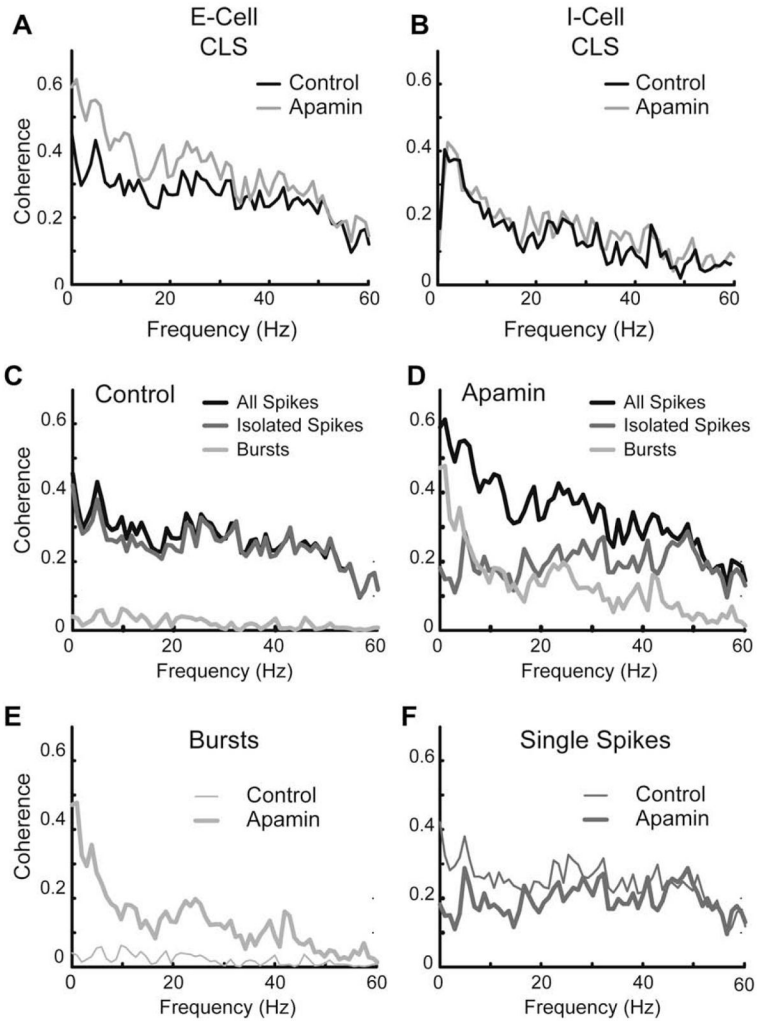

Fig. 5.

Apamin sensitive currents decrease response to low-frequency stimuli in E, but not I cells. Neurons in vitro were given a random amplitude modulation (RAM) current injection of 0–60 Hz Gaussian noise representative of naturalistic stimuli. (A) Coherence plot of a representative broadband CLS cell showing an increased response to low frequencies following apamin (gray). Neither I cells (B) nor CMS superficial cells (not shown) display frequency-response changes to the RAM following application of apamin (1 uM; grey). (C,D) Separation of the coherence response of the CLS cell from A under control conditions (C) and apamin (D) into components attributable to single spikes (medium gray) or bursts (light grey). (E) Overlay of burst component from C (thin trace) and D (thick trace) showing an increased burst response to low frequencies. (F) Overlay of the isolated spike component from C (thin trace) and D (thick trace) showing only minor response changes. Data from Ellis et al. (2007b).

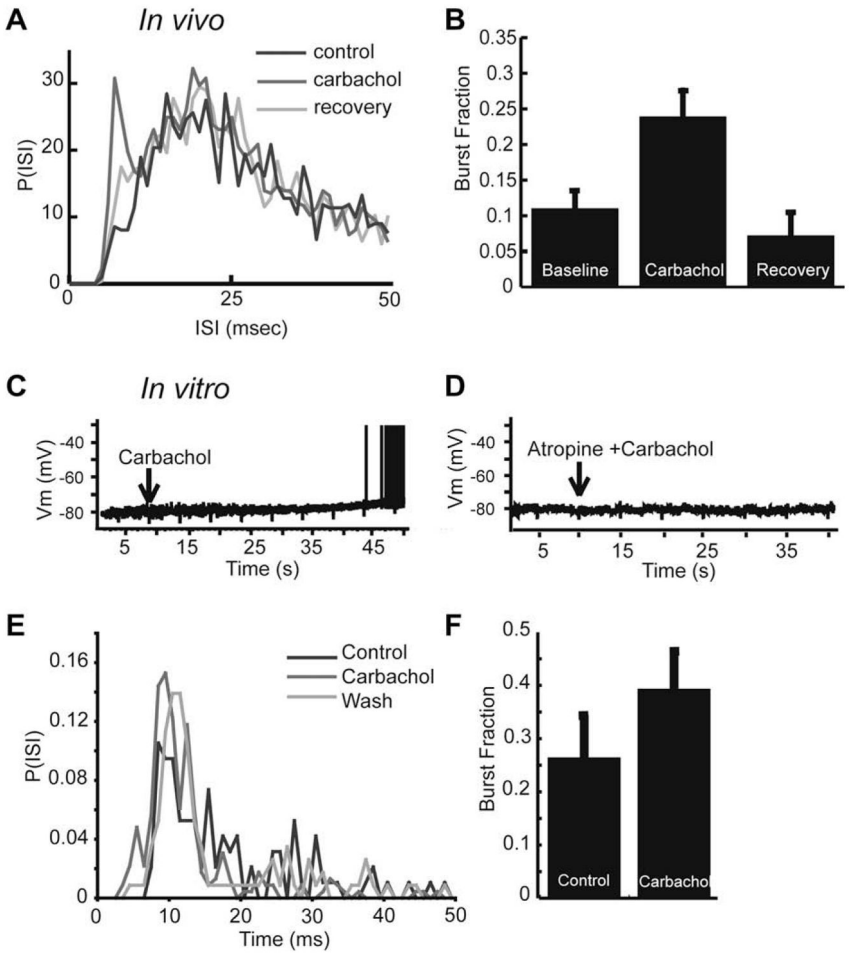

Fig. 6.

Muscarinic receptor activation leads to an increase in burst firing and low-frequency response in vivo and in vitro. Carbachol increases burst discharge in vivo. (A) ISI histograms before, during, and after, application of carbachol. Carbachol leads to an increase in the number of ISIs shorter than 10 ms. (B) Bar graph representing the average increase of the burst fraction in vivo (fraction of ISIs < 10 ms; control: 0.11 ± 0.10; carbachol: 0.24 ± 0.15) following carbachol and return to control levels following recovery period. (C) In vitro application of carbachol induced a slow depolarization of ELL pyramidal cells, and is sufficient to drive them to fire spikes. (D) Atropine eliminates the carbachol induced depolarization observed in vitro, suggesting mAChR activation. (E) ISI histogram showing an increase in ISI's < 10 ms following carbachol application in vitro. (F) An increase in the burst fraction is also observed in vitro (fraction of ISIs < 10 ms) after carbachol application. Modified from Ellis et al. (2007a).

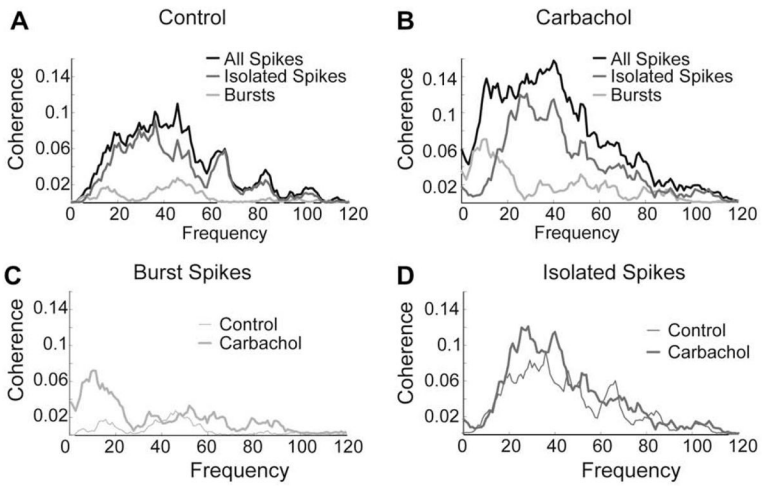

Fig. 7.

Muscarinic receptor activation increases the response to low-frequency sensory stimuli in vivo. (A) Under control conditions, the cell has very little low-frequency coherence, and rarely bursts. (B) After application of carbachol the low-frequency coherence increases for the entire spike train, but particularly for the burst spikes. (C) Much of the increase in low-frequency coherence is due to the increase in bursting. (D) A smaller fraction of the < 40 Hz increase is mediated by isolated spikes. Data is shown here for one representative cell.

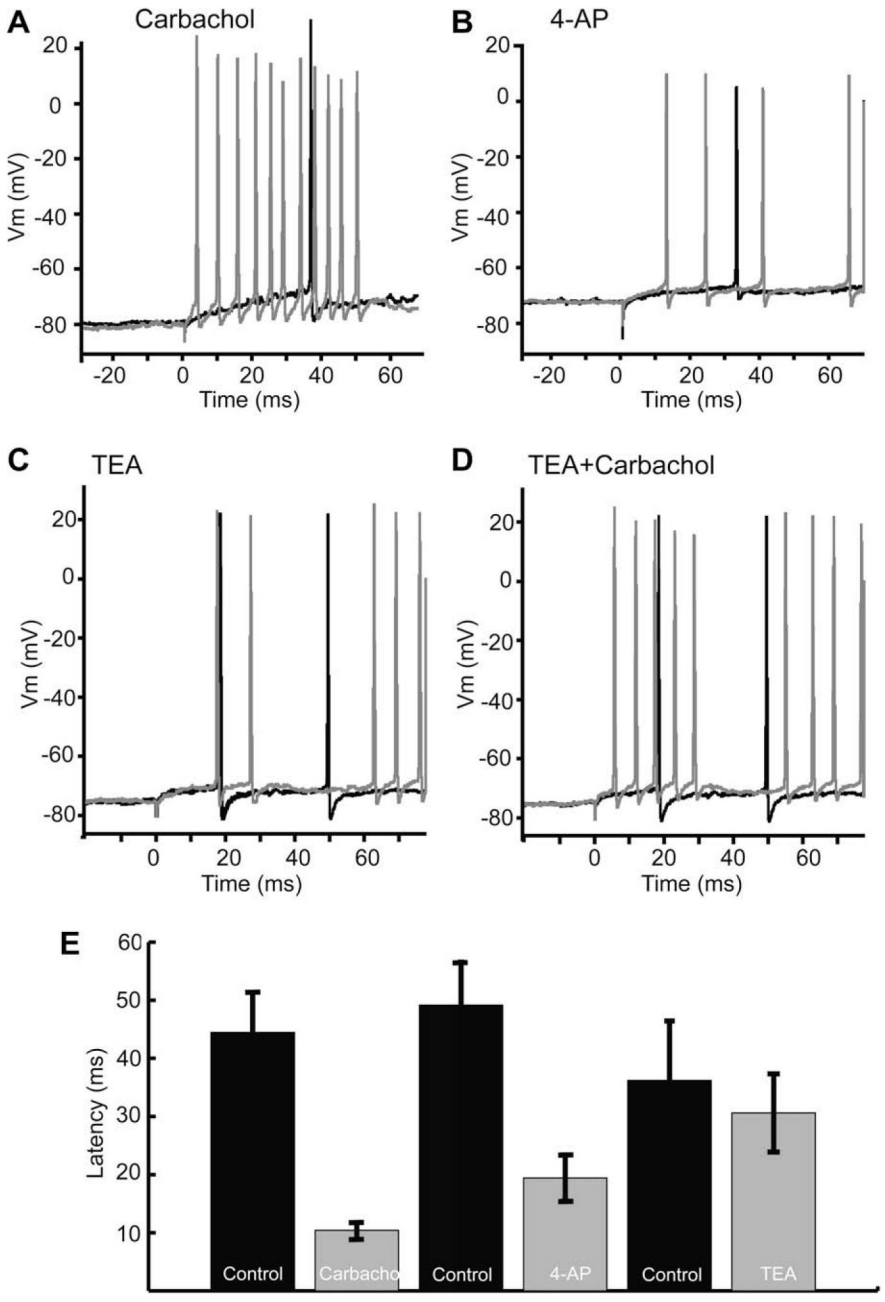

Fig. 8.

In vitro application of carbachol and 4-AP, but not TEA, leads to a decreased first spike latency, suggesting the involvement of a subthreshold A-type-like current. (A) Carbachol leads to a reduced spike latency following a step current injection (0.2 nA). (B) 4-AP mirrors the effect of carbachol reducing first spike latency in a representative cell. (C) TEA does not alter the spike latency. (D) Carbachol decreases latency even when applied after TEA. (E) Bar graphs showing a significant decrease in latency following carbachol and 4-AP, while TEA failed to cause a significant decrease in latency. Representative cells taken from Ellis et al. (2007a).

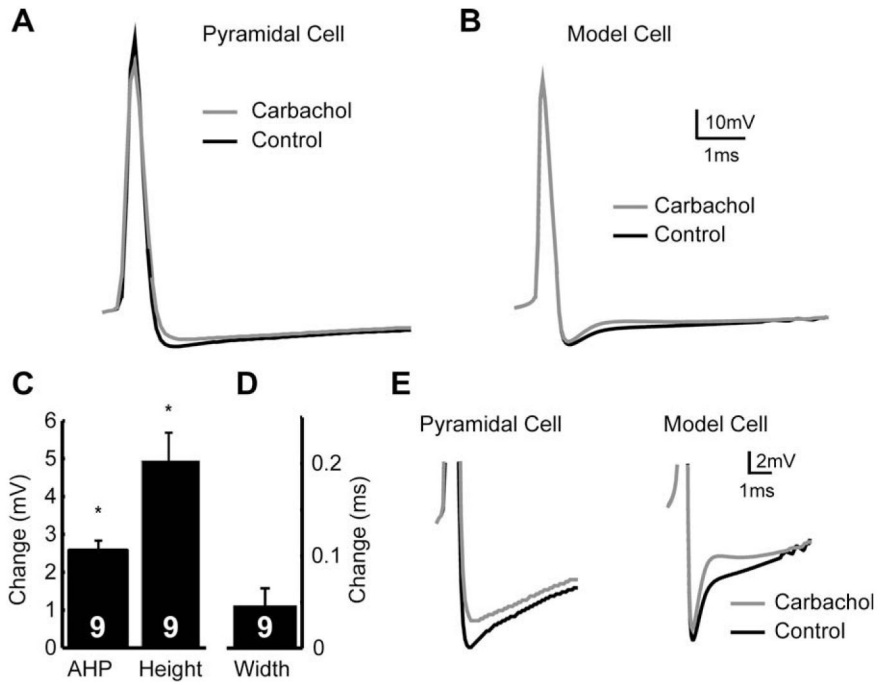

Fig. 9.

Carbachol regulates the AHP, which cannot be replicated by removal of an I_A current. (A) Representative spikes showing that application of carbachol reduces the AHP amplitude (grey line) relative to control (black line). (B) The removal of I_A from a reduced compartmental model can not replicate the decrease in AHP size. (C) Averages showing the changes in AHP size and spike height. (D) As shown by a representative cell, spike width was not significantly affected by carbachol. (E) Insets showing (A) and (B) in greater detail.

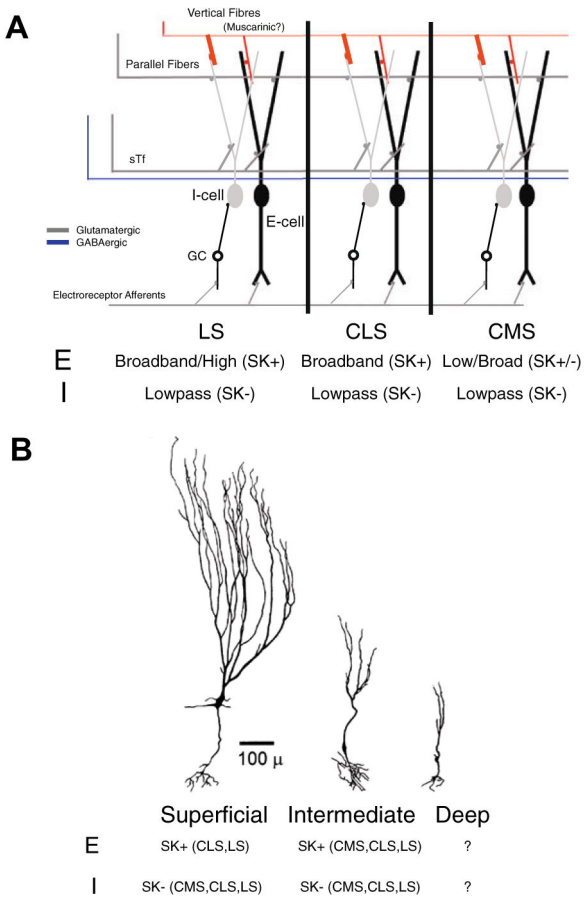

Fig. 10.

Pyramidal cell frequency tuning and equipment with SK channels varies with the segment and cell class. (A) Architecture of the ELL, with each of the three tuberous maps shown. Putatively, all three maps receive muscarinic inputs in the DML. The three maps differ in frequency selectivity and SK channels expression in E, but not I type pyramidal cells. (B) Within maps, SK expression can also vary. SK expression is apparent in CMS intermediate, but not superficial E cells. In the CLS and LS SK expression is apparent in both intermediate and superficial E cells. The expression pattern in deep pyramidal cells remains undetermined.